

Electron-impact excitation autoionization of helium in the S -wave limit

D. A. Horner,^{1,2} C. W. McCurdy,^{2,3} and T. N. Rescigno²

¹*Department of Chemistry, University of California, Berkeley, California 94720, USA*

²*Chemical Sciences, Lawrence Berkeley National Laboratory, Berkeley, California 94720, USA*

³*Department of Applied Science and Department of Chemistry, University of California, Davis, California 95616, USA*

(Received 23 September 2004; published 3 January 2005)

Excitation of the autoionizing states of helium by electron impact is shown in calculations in the S -wave limit to leave a clear signature in the singly differential cross section for the $(e, 2e)$ process. It is suggested that such behavior should be seen generally in $(e, 2e)$ experiments on atoms that measure the single differential cross section.

DOI: 10.1103/PhysRevA.71.010701

PACS number(s): 34.80.Dp

Doubly excited, autoionizing states of the helium atom have been the subject of numerous experimental and theoretical studies ever since the 1P states were detected in photoabsorption by Madden and Codling [1] some 40 years ago. These states, as well as additional optically forbidden states, were subsequently observed in electron impact studies by Simpson *et al.* [2] and there have since been numerous experimental studies of excitation autoionization. The process is generally regarded as occurring in two steps: excitation of the autoionizing state, followed by its decay. It was also realized quite early [3] that postcollision interactions between scattered and ejected electrons could complicate this simple picture. In any case, since it is not possible to distinguish electrons that have been ejected directly from an atom from those that are first promoted to an autoionizing state, the two processes will interfere, as shown by van den Brink *et al.* [4]. The observable consequences of this interference are pronounced changes in the energy and angular dependence of the ejected electrons in the vicinity of autoionization resonances [5].

Theoretical treatments of excitation autoionization have assumed that, for situations where one of the final state continuum electrons is near an autoionizing level, the ionization amplitude can be written as a sum of direct and resonant terms. The resonant part of the amplitude is frequently parametrized in terms of Shore or Fano parameters [6], whereas the direct or background component is generally approximated using a perturbative treatment, such as the plane-wave [7] or distorted-wave [8] Born approximations. Such treatments, not surprisingly, can be very sensitive to the model used for the direct ionization [9]. Our purpose here is to present the initial results of a completely nonperturbative treatment of the excitation autoionization of helium in the S -wave model. The S -wave model simplifies the full problem by treating only states with zero orbital angular momentum. While such a model cannot give a quantitatively accurate description of the full e^- -He ionization problem, it does represent a true four-body Coulomb problem and therefore shows much of the complexity associated with the full problem. In particular, we will show how doubly excited target states leave a clear signature in the single differential cross section (SDCS) for ionization, in which pairs of resonance peaks appear, symmetrically related by the energies of either the scattered or ejected electron, signaling the decay of an

autoionizing state. These peaks also provide a sensitive measure of postcollision interaction effects—a situation we expect will carry over to the full problem. Moreover, by using the method of exterior complex scaling (ECS) to compute the required wave functions, we are able to compute accurate ionization cross sections without having to make any *a priori* assumptions about the form of the ionization amplitudes.

Most of the recent theoretical work on e^- -He ionization using nonperturbative methods has been carried out with a single active electron model with one of the target electrons frozen in the $1s$ orbital of He^+ . Such a model is incapable of describing excitation autoionization, which requires two active target electrons. In our recent study of electron-He ionization in the S -wave model [10], we showed how the exterior complex scaling method could be applied to the full three-electron problem without invoking a frozen-core model. Plottke *et al.* [11] have also examined the S -wave model for e^- -He using the convergent close-coupling method. In the ECS method, the radial coordinates of the electrons are scaled beyond some point R_0 using the transformation $r \rightarrow R_0 + (r - R_0)e^{i\theta}$. This transformation allows one to solve for the scattered wave portion of the full wave function with the simple boundary condition that the solution vanish as $r \rightarrow \infty$ for any electron along the exterior scaling contour. This condition is formally equivalent to outgoing scattering boundary conditions (for producing the solution for $r < R_0$), even in the presence of long-range potentials, as has been discussed at length elsewhere [12].

In all applications of ECS to scattering problems, the full wave function Ψ^+ is partitioned into unperturbed and scattered wave components,

$$\Psi^+ = \Phi_0 + \Psi_{\text{SC}}, \quad (1)$$

which then yields a driven equation for the scattered wave

$$(E - H)\Psi_{\text{SC}} = (H - E)\Phi_0. \quad (2)$$

Expansion of the wave function on a grid using an appropriate discretization method (finite difference or finite elements) reduces Eq. (2) to a system of complex, linear equations. In the present study, the discretization was achieved by using Rescigno and McCurdy's combined finite element-discrete variable representation (FEM-DVR) [15]. With two radial electron coordinates, it is feasible to solve these equations

TABLE I. Energy levels for S -wave helium that are relevant to the results presented in this paper.

State	Energy (a.u.)= $E_r - i\Gamma/2$					
	ECS		Draeger <i>et al.</i> (Ref. [13]) ^a		Manby and Doggett (Ref. [14])	
$ksk's$	0					
$2sks$	-0.5		-0.5		-0.5	
$2s3s(^1S)$	-0.571 923	-0.28473(-3) i	-0.571 8819 5	-0.2820(-3) i	-0.571 495	-0.330 90(-3) i
$2s3s(^3S)$	-0.584 855	-0.90332(-6) i	-0.58 48547 7		-0.58481068	-0.95985(-6) i
$2s2s(^1S)$	-0.722 837	-0.11992(-2) i	-0.722 6508 1	-0.1205(-2) i	-0.722 281	-0.12205(-2) i
$1sks$	-2		-2			
$1s3s(^1S)$	-2.060 79		-2.060 79			
$1s3s(^3S)$	-2.068 49		-2.068 49			
$1s2s(^1S)$	-2.144 20		-2.144 19			
$1s2s(^3S)$	-2.174 26		-2.174 26			
$1s1s(^1S)$	-2.879 03		-2.879 03			

^aThe values given for the widths are the corrected values cited in Ref. [14].

directly. However, with three electron coordinates, even with zero orbital angular momentum for each electron, the size of the linear systems become very large and impractical to solve. We addressed this difficulty by recasting the problem with an equivalent time-dependent formulation [10,16] that does not require us to solve large linear systems.

The time-dependent formulation follows from noting that the solution of Eq. (2), which we seek, can be formally written as

$$\Psi_{SC} = -i \int_0^\infty e^{i(E+i\epsilon)t} \chi(t) dt, \quad (3)$$

where, under ECS, the “wave packet” $\chi(t) = e^{-iHt}(H-E)\Phi_0$ will limit to zero for large $\{r_j\}$ as $t \rightarrow \infty$, so the $+i\epsilon$ in Eq. (3) can be dropped. Equation (3) is thus formally equivalent to the solution of Eq. (2). Instead of solving large linear systems, it requires that we propagate $\chi(0)$ on the ECS contour in multiple dimensions for times sufficiently large to converge the Fourier transform that provides the numerical representation of Ψ_{SC} . We showed in Ref. [10], where further computational details are fully explained, that this formulation could be practically applied to the S -wave electron-He problem. Here we extend these calculations by considering collision energies where autoionizing states of the target atom can be excited. All of the computational parameters, such as the number and spacing of the finite elements, the order of the DVR, and the parameters of the time propagation, are identical to what was used in that earlier study.

We begin with a description of the bound and doubly excited target states relevant to this study. These can be found by diagonalizing the complex-scaled target Hamiltonian because the bound states are unaffected by the transformation and the doubly excited states naturally appear as eigenvalues of this Hamiltonian, with complex eigenvalues whose imaginary parts are equal to half the corresponding autoionization widths [17]. Table I shows the relevant states for the S -wave He target. Where possible, comparison is

made with the results of Draeger *et al.* [13], who used quantum defect theory to compute the energy positions and a numerical solution of coupled-channel scattering equations to obtain the widths, and Manby and Doggett [14], who used Feshbach theory. The values we found for the bound and autoionizing states were insensitive to changes in the rotation angle, the size of the grid, and the order of the DVR functions employed, so these calculations indicate they are correct to the number of figures given.

We now turn to the evaluation of scattering cross sections in the S -wave electron-He problem. The most practical approach to calculating both the excitation and breakup cross sections is to formulate the problem in terms of integral expressions for the underlying scattering amplitudes [18]. The amplitudes for discrete excitations can be readily computed by starting with the formal expression

$$f_{i \rightarrow n} = \frac{2}{\sqrt{k_n}} \langle \phi_n(r_1, r_2) \sin(k_n r_3) | E - H_1 | \Psi^+ \rangle, \quad (4)$$

where ϕ_n is a discrete target state and H_1 is the unperturbed Hamiltonian corresponding to the incident channel arrangement. We can then use Green's theorem to express the amplitude as a surface integral

$$f_{i \rightarrow n} = \frac{1}{\sqrt{k_n}} \int_S [\phi_n(r_1, r_2) \sin(k_n r_3) \nabla \Psi_{SC}(r_1, r_2, r_3) - \Psi_{SC}(r_1, r_2, r_3) \nabla \phi_n(r_1, r_2) \sin(k_n r_3)] \cdot d\hat{\mathbf{S}}, \quad (5)$$

where the replacement of Ψ^+ by Ψ_{SC} follows from an examination of the integrand of Eq. (5) on the surface.

The development of a workable expression for the single ionization amplitude on a finite volume is more difficult. The following expression for the ionization amplitude:

$$f(k_1, k_2) = 2 \langle \varphi_{k_1}^{(c)}(r_1) \varphi_{k_2}^{(c)}(r_2) \varphi_n(r_3) | E - H_1 | \Psi_{SC} \rangle, \quad (6)$$

where $\varphi_k^{(c)}$ is a Coulomb function and φ_n is a bound He⁺ orbital, while formally correct, is not useful on a finite vol-

ume. The problem is that the scattered wave contains asymptotic terms arising from both discrete excitations and ionization, and the discrete terms contaminate the evaluation of the ionization amplitude when the integration is carried out on a finite volume. While we have yet to find a perfect solution to this problem, we have shown that useful results can be obtained by making a judicious choice of distorted waves to represent the final continuum electrons and by using the technique of “asymptotic subtraction” to remove the asymptotic contribution of the discrete two-body channels to the scattered wave before computing the ionization amplitude. Details can be found in Ref. [10].

When the incident electron energy is high enough to promote the target to a doubly excited state, then one expects to find structure in the energy sharing or single differential cross section for ionization at ejected electron energies corresponding to the decay of the autoionizing state. Whether such a structure is observable depends on the probability of exciting the resonance state relative to the total ionization probability. To get some idea of the magnitude of these effects, we first computed the excitation cross sections to the doubly excited states, using the amplitudes given by Eq. (4), as if the resonance states were bound excited states. For this purpose, we obtained unit normalized target states by diagonalizing the real target Hamiltonian on a small (~ 40 bohr) box. We calculated excitation cross sections for the $2s2s(^1S)$, $2s3s(^3S)$, and $2s3s(^1S)$ states, starting from the ground state and as well as from the $1s2s(2^{1,3}S)$ and $1s3s(3^{1,3}S)$ excited states at a few energies near threshold. This allows us to define ratios between excitation and total ionization cross sections, $R \equiv \sigma_{excit}/\sigma_{ion}$. Starting from the ground state, the R value we found for exciting the $2s2s(^1S)$ state was less than one part per thousand, which is in fact very similar to the values one would calculate for the physical problem using measured values for the $2s2s(^1S)$ excitation [3] and total ionization [19] cross sections. Because of small computational errors in our calculated SDCS that arise, as we have stated above [10], from our inability to completely remove the contamination from discrete excitation channels, we could not reliably resolve any autoionization structures in the ground-state ionization cross sections. However, the R values we computed for exciting the $2s2s(^1S)$ and $2s3s(1^{3,3}S)$ states starting from *excited* target states— 2^1S , 2^3S , 3^1S , and 3^3S —were significantly larger, on the order of several percent, and for these cases, excitation-ionization resonances in the SDCS could be readily identified.

Figure 1 shows the SDCS from the 2^3S state at incident electron energies of 37.0 and 44.0 eV. At the lower energy, which is ~ 2.5 eV below the energy required to excite the $2s2s(^1S)$ autoionizing state, we find the usual bow-shaped SDCS, while at 44.0 eV, the SDCS shows two sharp peaks, symmetrically positioned with respect to $E/2$ as they must be, at energies for either scattered or ejected electron corresponding to the decay of the $2s2s(^1S)$ autoionizing state. In fact, because of postcollision interactions, there is a shift of ~ 0.25 eV between the unperturbed energy of the autoionizing electron and the energy at which the peak appears in the SDCS. This effect is further illustrated in Fig. 2, where we plot the SDCS, from both the 2^3S and 2^1S initial states, for

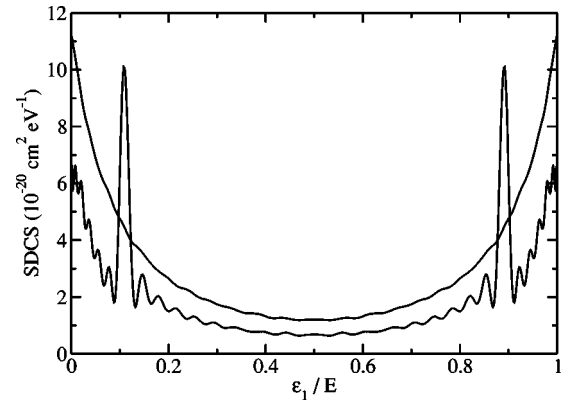


FIG. 1. SDCS for ionization from the 2^3S state at 37.0 eV (upper curve) and 44.0 eV (lower curve) incident electron energy, showing the characteristic symmetric appearance of autoionizing features in the SDCS, in this case due to the $2s2s(^1S)$ state.

ejected electron energies near those corresponding to the decay of the $2s2s(^1S)$ autoionizing state, as a function of incident electron energy. The calculations clearly show that as the incident energy increases, the magnitude of the peaks decrease as they shift closer to the unperturbed energy of the doubly excited target state. The effects of the postcollision interaction are expected to decrease with increasing incident energy above the excitation energy for the autoionizing state, and Fig. 2 shows exactly that effect.

Figure 3 shows similar results for the 3^3S and 3^1S initial states, in this case for ejected electron energies near those corresponding to the decay of the $2s3s(^1S)$ autoionizing state. We note the widths of the resonance features seen in the SDCS are similar to those seen in Fig. 2 for the $2s2s(^1S)$ autoionizing state despite the fact that the $2s3s(^1S)$ autoionizing state has an intrinsic width that is about four times smaller than the width of the $2s2s(^1S)$ state.

The widths of the doubly excited states do appear to correlate with the number of steps in our time propagation scheme required to converge the autoionization features in

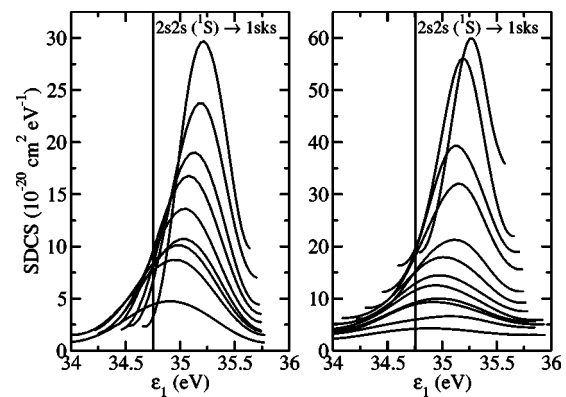


FIG. 2. SDCS for ionization from the 2^3S (left) and 2^1S (right) states, for various incident electron energies, at ejected electron energies near the decay of the $2s2s(^1S)$ resonance state. For the 2^3S case, incident energies are (top to bottom) from 41.0 to 45.0 eV in increments of 0.5 eV. For the 2^1S case, the energies are from 39.5 to 45.0 eV in increments of 0.5 eV.

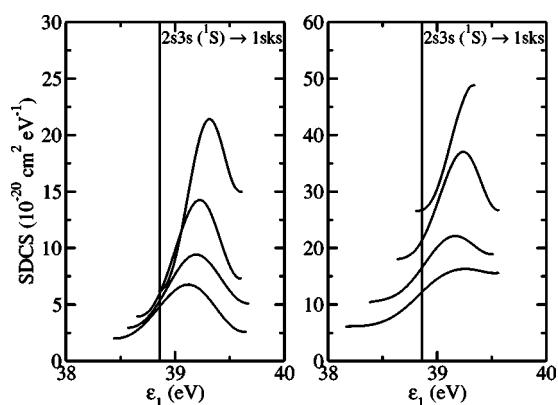


FIG. 3. SDCS for ionization from the 3^3S (left) and 3^1S (right) states, for various incident electron energies, at ejected electron energies near the decay of the $2s3s(^1S)$ resonance state. For the 3^3S case, incident energies are (top to bottom) from 41.5 to 43.0 eV in increments of 0.5 eV. For the 3^1S case, the energies are from 41.0 to 42.5 eV in increments of 0.5 eV.

the SDCS. In the case of the 2^3S and 2^1S initial state calculations, we found that the initial wave packets had to be propagated for ~ 300 atu to converge the $2s2s(^1S)$ peaks in the calculated SDCS. However, to obtain similar convergence for the $2s3s(^1S)$ peaks seen in the 3^3S and 3^1S initial states ionization cross sections required propagation times of

~ 1000 atu. This scaling would indicate that propagation times on the order of half a million atu, which are completely impractical, would be required to see peaks corresponding to the $2s3s(^3S)$ doubly excited state. This undoubtedly explains why we have not seen peaks corresponding to this state in any of our calculated SDCS.

In summary, we have presented nonperturbative calculations of electron-helium ionization in the S -wave model that clearly show structure in the SDCS corresponding to excitation ionization. In this model, the structures are seen in the cross sections for ionization, starting from excited helium target states. The peaks in the SDCS initially appear at ejected electron energies slightly greater than those corresponding to the decay of the doubly excited states, in agreement with experimental observation [3]. Our calculations suggest that such peaks should be seen in the experimental SDCS for cases where the cross section for exciting the autoionizing states are large enough to appear above the background of direct ionization.

This work was performed at the University of California Lawrence Berkeley National Laboratory under the auspices of the U.S. Department of Energy, under Contract No. DE-AC03-76SF00098, and was supported by the U.S. DOE Office of Basic Energy Sciences, Division of Chemical Sciences. D.H. also acknowledges support from the U.S. DOE Computational Science Graduate program.

-
- [1] R. P. Madden and K. Codling, *Phys. Rev. Lett.* **10**, 516 (1963).
 - [2] J. A. Simpson, G. E. Chamberlain, and S. R. Mielczarek, *Phys. Rev.* **139**, A1039 (1965).
 - [3] D. Spence, *Phys. Rev. A* **12**, 2353 (1975).
 - [4] J. P. van den Brink, J. van Eck, and H. G. M. Heideman, *Phys. Rev. Lett.* **61**, 2106 (1988).
 - [5] D. G. McDonald and A. Crowe, *J. Phys. B* **25**, 4313 (1992).
 - [6] R. J. Tweed, *J. Phys. B* **9**, 1725 (1976).
 - [7] V. V. Balashov, S. S. Lipovetsky, and V. S. Senashenko, *Zh. Eksp. Teor. Fiz.* **63**, 1622 (1972), [*Sov. Phys. JETP* **36**, 858 (1973)].
 - [8] A. Pochat, R. J. Tweed, M. Doritch, and J. Peresse, *J. Phys. B* **15**, 2269 (1982).
 - [9] I. E. McCarthy and B. Shang, *Phys. Rev. A* **47**, 4807 (1993).
 - [10] D. A. Horner, C. W. McCurdy, and T. N. Rescigno, *Phys. Rev. A* **71**, 012701 (2005).
 - [11] C. Plotke *et al.*, *Phys. Rev. A* **65**, 032701 (2002); *J. Phys. B* **37**, 3711 (2004).
 - [12] C. W. McCurdy, M. Baertschy, and T. N. Rescigno, *J. Phys. B* **37**, R137 (2004).
 - [13] M. Draeger, G. Handke, W. Ihra, and H. Friedrich, *Phys. Rev. A* **50**, 3793 (1994).
 - [14] F. R. Manby and G. Doggett, *J. Phys. B* **30**, 3342 (1997).
 - [15] T. N. Rescigno and C. W. McCurdy, *Phys. Rev. A* **62**, 032706 (2000).
 - [16] C. W. McCurdy, D. A. Horner, and T. N. Rescigno, *Phys. Rev. A* **65**, 042714 (2002).
 - [17] W. Reinhardt, *Annu. Rev. Phys. Chem.* **33**, 223 (1982).
 - [18] C. W. McCurdy and T. N. Rescigno, *Phys. Rev. A* **62**, 032712 (2000).
 - [19] R. G. Montague, M. F. A. Harrison, and A. C. H. Smith, *J. Phys. B* **18**, 125 (1985).